*Earth Planets Space*, **55**, 301–313, 2003

# Effective skin depth of EM fields due to large circular loop and electric dipole sources

Nagendra Pratap Singh and Toru Mogi

*Institute of Seismology and Volcanology, Hokkaido University, N10W8 Kita-ku, Sapporo 060-0810, Japan*

(Received October 1, 2002; Revised May 1, 2003; Accepted June 10, 2003)

Definition and concept of plane wave skin depth is applied to study the effective skin depth due to large circular loop and horizontal electric dipole sources, and attempt is made to illustrate its application to the real field survey design and data interpretation problems. The effective skin depth, the depth at which the amplitude of a frequency-domain electromagnetic field due to a large circular loop source or an electric dipole source falls to $1/e$ of its value at surface of a homogeneous half space, is compared with the usual plane wave skin depth for variation of different survey and model parameters, viz. source frequency, source moment or loop dimension, source-receiver offset and half space conductivity. The results show their characteristic variations, and depict that the effective skin depth due to large loop source and/or electric dipole source depends on source-frequency, source moment, source-receiver offset and half-space conductivity. The effective skin depth may vary from a fraction of plane wave skin depth in near vicinity of the source to more than twice the plane wave skin depth at points away from the source. However, for large source-receiver offsets and/or high source frequencies and half-space conductivities, it tends to the plane wave skin depth. For receiver positions in near vicinity of the source, the effective skin depth curves exhibit variations specific to the source, and show different characteristic variations for different sources, whereas for receiver positions away and far away from the source, the effective skin depth curves show similar characteristic variations for all sources, irrespective of nature and geometry of the source. The results depict distinctive effect of geometry and nature of the source on effective skin depth. The examples presented for illustrating the application of effective skin depth depict that effective skin depth has direct relation with the EM response of the local source over the layered earth and thus, can be used as an aid for estimating the optimum parameters in EM survey design and data interpretations.

**Key words:** Electromagnetic response, skin depth, depth of investigation, circular loop source, electric dipole source.

## 1. Introduction

Estimation of depth of investigation of an electromagnetic (EM) system is very much crucial for both survey design and data interpretation. Theoretically, the EM field at any frequency is present at all the depths, albeit at vanishingly small level. The practical depth of investigation from geophysical standpoint depends on factors such as the sensitivity and accuracy of instruments, complexity of geologic section and the inherent noise level (Spies 1989). For estimating the depth of investigation in layered earth sections, a number of methods based on different approaches have been suggested by many earth scientists (e.g. Keller, 1971; Bostick, 1977; Parker, 1982; Spies, 1989; Reid and Macnae, 1999). The method relating skin depth to effective depth of penetration of EM fields in the earth (Bostick, 1977), and the effective skin depth (Reid and Macnae, 1999) are based on the concept of skin depth. The skin depth is the term related to propagation of plane wave EM field, and is commonly used to estimate the depth of investigation of an EM prospecting system. The skin depth, $\delta$ is defined as the depth at which the amplitude of the plane-wave electric or magnetic field in a homogeneous half-space falls to $1/e$ (nearly 37%) of its surface value (Stratton, 1941), while the phase rotates by one radian (Spies, 1989). Mathematically, it is given by

$$\delta = \sqrt{\frac{2}{\sigma \mu \omega}}, \tag{1}$$

where $\sigma$ is the half-space conductivity, $\omega$ $(=2\pi f)$ is the angular frequency, and $\mu$ is the magnetic permeability. The effective skin depth is analogous to the plane wave skin depth for the EM field of a finite source, which is not an ideal plane wave but can be represented as superposition of plane-wave solutions with varying, complex angles of incidence. Thus, the effective skin depth $\delta_e$ can be defined as the depth at which the amplitude of the electric or magnetic field of a local finite source in a homogeneous half-space reduces to $1/e$ of its surface value. This is also termed as local source skin depth (LSSD) by Reid and Macnae (1999).

Further, in accordance with definition of skin depth, for a given conductivity and permeability of the half space, the plane-wave skin depth depends mainly on frequency and is unique for a particular source frequency. This gives an idea about the depth of investigation of an EM system employing characteristic source frequency.

Reid and Macnae (1999) have applied the concept of plane

wave skin depth to the study of local source skin depth due to vertical and horizontal magnetic dipole and square loop sources. In their study, they have emphasis on magnetic dipole sources, and presented only a single result for the square loop source for source-receiver offsets outside and away from the loop in context with the dipole results, and as expected, they observed similar variation as that for a vertical magnetic dipole source. However, in case of a large loop source, one is mainly interested in the measurement of EM response in near vicinity of the source at points inside as well as outside the source loop, because of less power requirement, economy and convenience in measuring in close proximity of the loop. Thus, it is more useful and natural to have an idea about the effective skin depth due to a large loop source in near vicinity of the source at points inside as well as outside the loop than at points too away from the loop. Further, the EM methods employing magnetic dipole sources may be suitable for detecting relatively conductive layers, but for detecting a relatively resistive layers, which are of great importance in many practical cases, such as in exploration of oil saturated zone, one may require EM methods using electric dipole or other EM sources. Moreover, there must be some characteristic behavior of effective skin depth specific to each source, because in close proximity of the source, the EM field varies according to different rules for different sources. So, it would be informative and interesting to have an idea about the effective skin depth of EM fields due to electric dipole sources, constituting a wide class of EM sources. Thus, we perform a study about the effective skin depth of EM fields due to two sources: 1) a large circular loop (with receiver at points inside as well as outside the loop), and 2) a horizontal electric dipole. We compare the effective skin depth with the plane wave skin depth, for variation of several survey and model parameters, such as, source-receiver offset, source frequency, source moment or loop dimension, and half-space conductivity. An attempt is made to illustrate its application to survey design and data interpretation.

## 2. Theory and Methodology

### 2.1 Theoretical background

The expressions of EM fields at points at the surface and within a layered earth, due to horizontal circular loop and horizontal electric dipole sources are discussed in Ward and Hohmann (1988) and Wait (1982) respectively. The effective skin depth ($\delta_e$) at several receiver positions is estimated from the amplitude of electric and magnetic fields at points within a homogeneous half space. The relevant expressions for total electric ($E_\phi$) and magnetic ($H_z$) field components at a point within a half-space of conductivity ($\sigma_1 = \sigma$), permeability ($\mu_1 = \mu_0$) and permittivity ($\varepsilon_1 = \varepsilon_0$), due to a large horizontal circular loop of radius '$a$', carrying a current $Ie^{i\omega t}$ and placed on the surface of the half-space can be given as

$$E_\phi = -i\mu_0\omega Ia \int_0^\infty \frac{\lambda}{(u_0+u_1)} e^{-u_1 z} J_1(\lambda r)\, J_1(\lambda a)\, d\lambda, \quad (2)$$

and,

$$H_z = Ia \int_0^\infty \frac{\lambda^2}{(u_0+u_1)} e^{-u_1 z} J_0(\lambda r)\, J_1(\lambda a)\, d\lambda, \quad (3)$$

where $z$ is depth of the measurement point below the surface, $r = \sqrt{x^2+y^2}$ is the radial source-receiver offset, $u_n = \sqrt{\lambda^2 + k_n^2}$, and $k_n^2 = -i\omega\mu_0\sigma_n + \varepsilon_0\mu_0\omega^2$ for $n = 0, 1$, and $J_0$ and $J_1$ are the Bessel functions of first kind and orders 0 and 1. In these expressions, the harmonic factor $e^{i\omega t}$ is implied and SI units are used everywhere.

The corresponding expression for the vertical magnetic field ($H_z$) due to a horizontal electric dipole of length '$ds$', carrying a current $Ie^{i\omega t}$ and lying on surface of the half-space, at a point within the half-space and in the plane normal to the dipole can be written as

$$H_z = \frac{Ids}{4\pi} \int_0^\infty \frac{2\lambda^2}{(u_0+u_1)} e^{-u_1 z} J_1(\lambda r)\, d\lambda. \quad (4)$$

### 2.2 Methodology

The geometry for calculation of subsurface field due to the large circular loop source and horizontal electric dipole (lying on surface of the earth) are shown in Fig. 1(a) and (b). In Fig. 1(a), the points $P_1$, $P_2$ and $P_3$ denotes several receiver positions inside as well as outside the source loop. The calculation of the effective skin depth due to large circular loop and horizontal electric dipole sources at various receiver locations are performed using the expressions of $E_\phi$ and $H_z$ field components given by Eqs. (2)–(4). The computation of infinite integrals occurring in the expressions of field components are accomplished by converting these integrals into the corresponding Hankel transforms of order 0 and 1. Thereafter, for computing Hankel transforms, we have used the filter coefficients of Guptasarma and Singh (1997). For facilitating rapid convergence of the integrals, the kernels associated with these integrals have been checked for their convergence, and in case of slow convergent or divergent nature they were made convergent by subtracting or adding a convergent integral expression inside the integral sign and subsequently adjusting it or its equivalent analytic expression outside the integral sign, as described in Singh and Mogi (2003).

In order to determine the effective skin depth in a homogeneous half space, due to the horizontal large circular loop or electric dipole source at various receiver positions, we have calculated the total electric ($E_\phi$) and/ or magnetic ($H_z$) fields on regular rectangular grids within the half-space and then determined the depth at which their amplitude falls off to $1/e$ of its value at the surface. The grid intervals used in this computation are 0.05 m for the vertical ($z$-direction), and 5 m for $r \leq 1000$ m and 60 m for $r \geq 1000$ m for the horizontal direction. The entire process is embodied in such a suitable algorithm that it starts with the initial value of horizontal distance and depth, normally ($x = 0, z = 0$), then computes the field at regular increment of the depth and compares it for the skin depth criterion before the next increment until it attains the actual skin depth value. Thereafter, it takes next value of $x$ and repeats the same process. This process is repeated un-

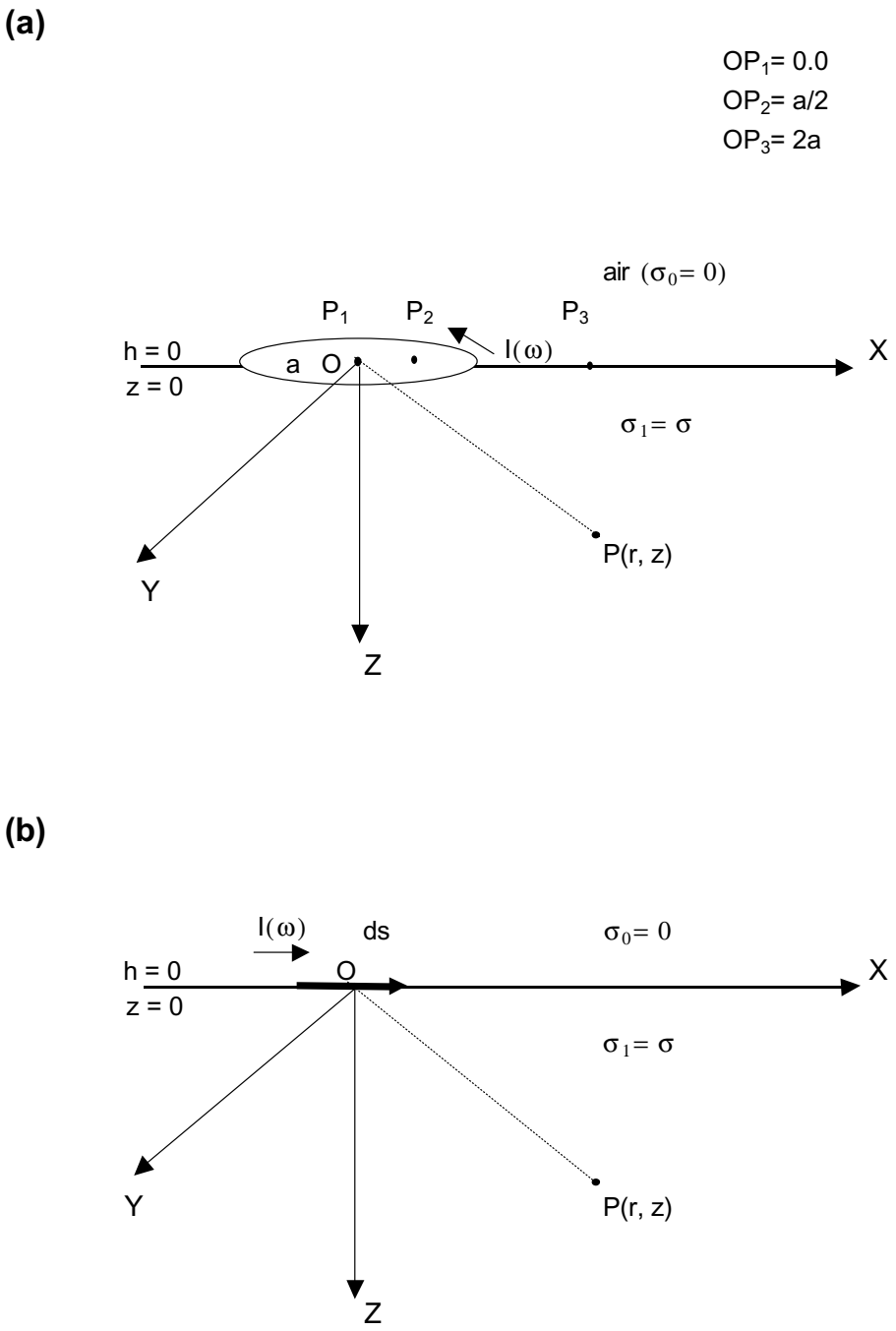


Fig. 1. Geometry of earth model and measurement system for calculation of EM fields and effective skin depth due to (a) large circular loop source, and (b) horizontal electric dipole source.

til we get the values of the skin depth for the desired profile length.

Unlike the plane wave skin depth ($\delta$), the effective skin depth ($\delta_e$) for a local source based on electric or magnetic field components may be different and even dual valued for some field components and survey geometries. Reid and Macnae (1999) have observed such non-uniqueness for the local source skin depth due to a horizontal magnetic dipole source, whereas Pridmore (1978) observed that for a vertical magnetic dipole (VMD) source, the $\delta_e$ based on electric field amplitude is uniquely defined because the electric field amplitude either decreases monotonically with depth or initially increases and then decreases to $1/e$ of its surface value. A non-unique $\delta_e$ is of little importance. The foremost criteria for getting a uniquely defined $\delta_e$ is that it should be based on those electric and/or magnetic field amplitudes, which either monotonically decreases with depth or initially increases before decreasing to $1/e$ of its surface. Therefore, with view of getting uniquely defined $\delta_e$, we have opted to calculate the $\delta_e$ due to large circular loop source on the basis of horizontal electric field computations, and have used the vertical magnetic field computations only for the position at center of the loop where the electric field expression does not exist. Further, for the case of horizontal electric dipole, we have opted to compute the $\delta_e$ using the vertical magnetic field due to the fact that for stratified earth, the vertical magnetic field gener-

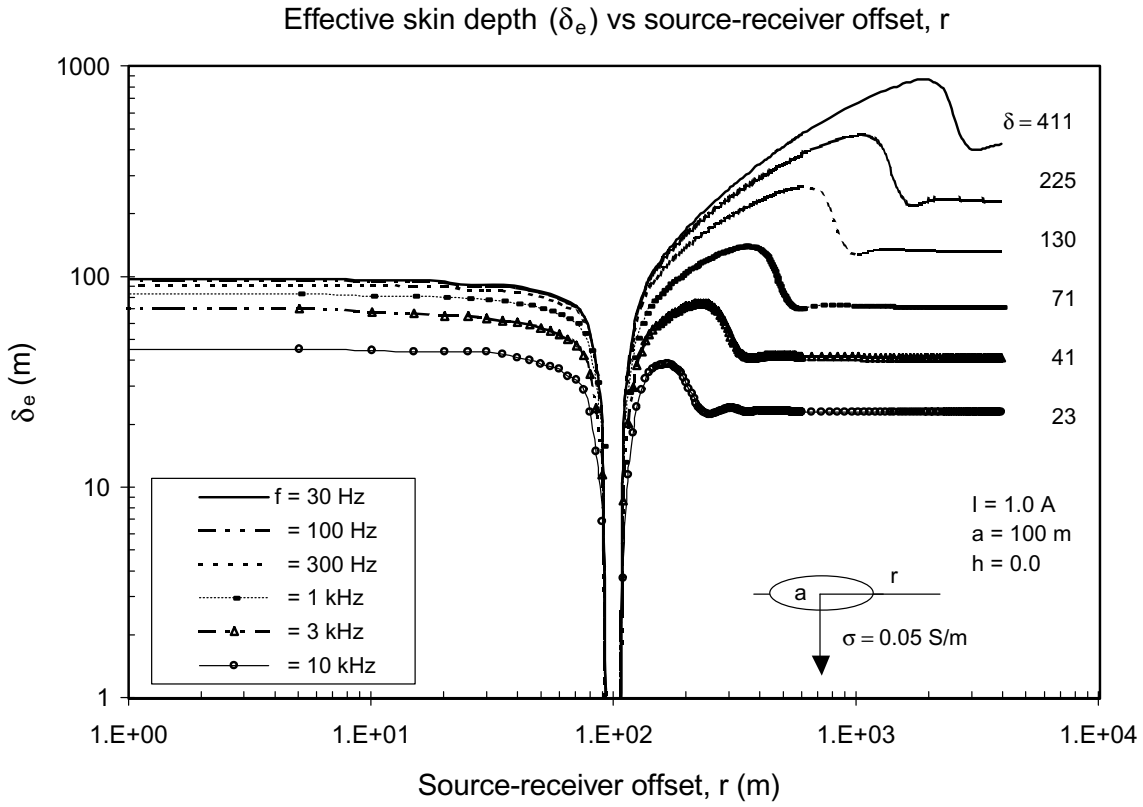


Fig. 2. Variation of effective skin depth, $\delta_e$ with source-receiver offset, $r$, for horizontal circular loop source of radius 100 m (carrying a unit current) for selected frequencies and model parameters as shown in the figure.

ated by a horizontal electric dipole either monotonically decreases with depth or initially increases and then decreases with depth (Kaufman and Hoekstra, 2001). In our computations, we did not come across any non-uniqueness problem.

## 3. Results and Discussions

### 3.1 Effect of survey and model parameters on $\delta_e$

In order to study the effect of variation of survey and model parameters on the effective skin depth due to a local source, we have computed $\delta_e$ due to horizontal large circular loop and electric dipole sources for several source-receiver offsets, and with different frequencies, source loop dimensions, and half-space conductivities. The resulting curves are plotted for profiles through the center of the loop or normal to the electric dipole. The source-receiver offset is measured from the center of the loop or from the center of the electric dipole, in a plane perpendicular to the dipole direction.

Figure 2 shows variation of effective skin depth due to a large circular loop source of radius, $a = 100$ m placed on the surface of a homogeneous half-space of conductivity ($\sigma = 0.05$ S/m) with horizontal source-receiver offset ($r = \sqrt{x^2 + y^2}$) for some selected source frequencies in the range 30 Hz to 10 kHz and other parameters as shown in the figure. The plane wave skin depth, $\delta$ at each frequency is indicated for each curve in the figure. From Fig. 2, it is obvious that $\delta_e$ curves show similar characteristic variation for all frequencies. The variation of $\delta_e$ with source-receiver offset can be described as follows: for very small values of source-receiver offset, $r$ (i.e. at $r \approx 0$) each curve has a $\delta_e$ smaller than the loop radius, it is smaller than $\delta$ for the lower frequencies (30, 100, 300 Hz) and larger than $\delta$ for the higher frequencies (1, 3, 10 kHz). The curve maintains almost constant value for $0 < r < \frac{2}{3}a$. When $r \to a$, it takes a further lower value and becomes infinitesimally small. At $r = a$, its value is un-determined. Thereafter, as $r$ increases, $\delta_e$ increases and attains its maximum value (more than twice the plane wave skin depth) for a value of $r$ depending upon the source frequency. For higher frequencies, the maximum is attained at comparatively smaller source-receiver offsets as compared to those for the lower frequencies. Finally, for large to very large values of source-receiver offset ($r > 10\delta$), the curve approaches to its plane wave skin depth value. A sharp variation in $\delta_e$ near the loop circle may be due to the reason that for small distances from the loop (circle) either inside or outside the loop, geometrical effects dominates over the natural dispersive effects responsible for skin depth (i.e. primary field fall-off is more dependent upon the nature and geometry of the source than it is on the EM dispersion). The un-determined value of $\delta_e$ at the circle of the loop is due to divergence of the $E_\phi$ field expression at that point. The variation of $\delta_e$ in near vicinity of the loop can be regarded as characteristic feature of large loop sources.

Figure 3 presents variation of the normalized effective skin depth ($\delta_e/\delta$) with induction number ($B = r/\delta$) for different loop sizes and other parameters as shown in the figure. From figure, it is observed that for small induction number, $\delta_e/\delta$ has a value ranging from a fraction of unity (for small loop sizes) to more than unity (for large loop sizes). With increase in induction number, it decreases and reaches to its lowest in close vicinity of the loop circle. Thereafter, with increase in

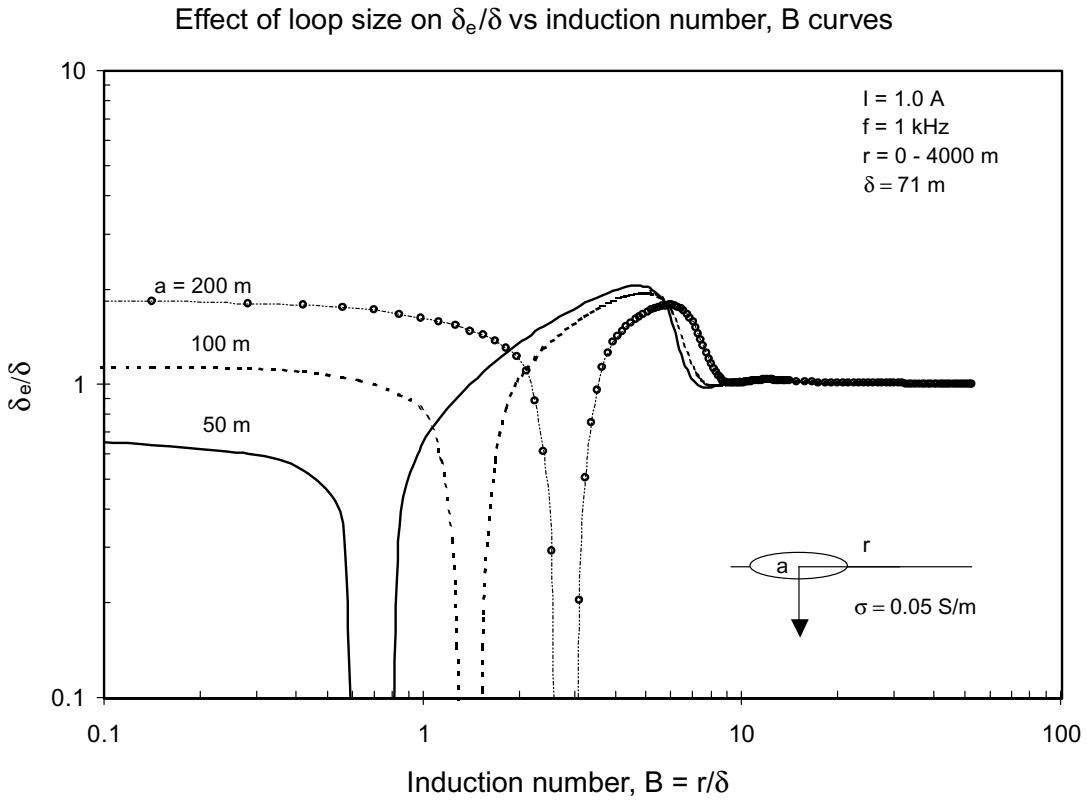


Fig. 3. Normalized effective skin depth, $\delta_e/\delta$ versus induction number, ($B = r/\delta$) curves for varying loop size and model parameters as shown in the figure.

induction number, it increases and reaches to its maximum, and finally, at very large induction numbers it converges to unity. With increase in loop dimension, the $\delta_e$ increases in general, and in particular in the region $r < a$ (i.e. in region where the source-receiver offset is less than radius of increased source loop) due to the fact that increasing the loop dimension, the magnetic moment of source increases resulting in a deeper skin depth value. Though, the absolute magnitude of the field increases with increasing transmitter moments, the maximum value of $\delta_e$, which is reached outside the source loop decreases slightly with increasing loop size. This may be due to the fact that on a profile through the center of the loop both front and back portion of the loop along the profile contribute to the tangential electric field and thus, the local source skin depth may be regarded as an average of their contributions. Therefore, for moderately large offsets ($r \approx 2\delta - 6\delta$), though the front portion of the loop remains at moderately close to the receiver but the back portion becomes away from the receiver and the average results in a decrease in the maximum $\delta_e$.

Figure 4(a) presents $\delta_e/\delta$ versus frequency curves for a circular loop source for an in-loop point at source-receiver offset, $r = 0$ (i.e. receiver at center of the loop) for different loop sizes and model parameters as shown in the figure. From Fig. 4(a), it is obvious that all the curves show similar variation for each loop size. For low frequencies, $\delta_e$ is smaller than $\delta$. With increase in frequency, $\delta_e$ increases and reaches to its maximum value, about $2.1\delta$ for medium to high frequencies, and finally converges to $\delta$ for high to very high frequencies depending upon the source loop size. With increase in loop dimension, the curves shift toward the lower frequency region. The maximum value of $\delta_e/\delta$ decreases slightly with increase in loop dimension, viz. for a loop radius $a = 50$ m, $\delta_e/\delta = 2.101$, while for $a = 400$ m it is 2.097. From Fig. 4(b), showing the variation of $\delta_e/\delta$ versus half-space conductivity for selected frequencies 100 Hz and 1000 Hz, it is observed that curves are similar in trend to the $\delta_e/\delta$ versus frequency curves. For low conductivity values, $\delta_e$ is much less than $\delta$. With increase in conductivity $\delta_e$ increases and reaches to its maximum value, about $2.1\delta$ for moderate conductivity values, and finally it converges to $\delta$ for high conductivity values. The effect of frequency variation is well reflected and with increase in frequency the curves appear to be shifted towards the lower conductivity region.

Figure 5(a) presents $\delta_e/\delta$ versus frequency curves for varying loop sizes, and Figure 5(b) presents $\delta_e/\delta$ versus half-space conductivity curves for frequencies 100 Hz and 1000 Hz respectively, for an offset loop point at source-receiver offset, $r = 2a$ and model parameters as shown in the figures. From Figs. 5(a) and (b), it is observed that curves in both the figures show similar characteristic variations. These curves show a small peak ($\sim 2\delta$) followed by the main peak ($\sim 2.2\delta$), which appears shifted towards the lower frequency range for increasing loop size. The second peak may be due to the result of combined geometric and dispersion effects, and/or due to the computational error resulting from the computation of Bessel function using the subprogram $bessj1(x)$ (Press *et al.*, 1992), which uses an approximate expression for large arguments ($x > 8$). With increase in loop dimen-

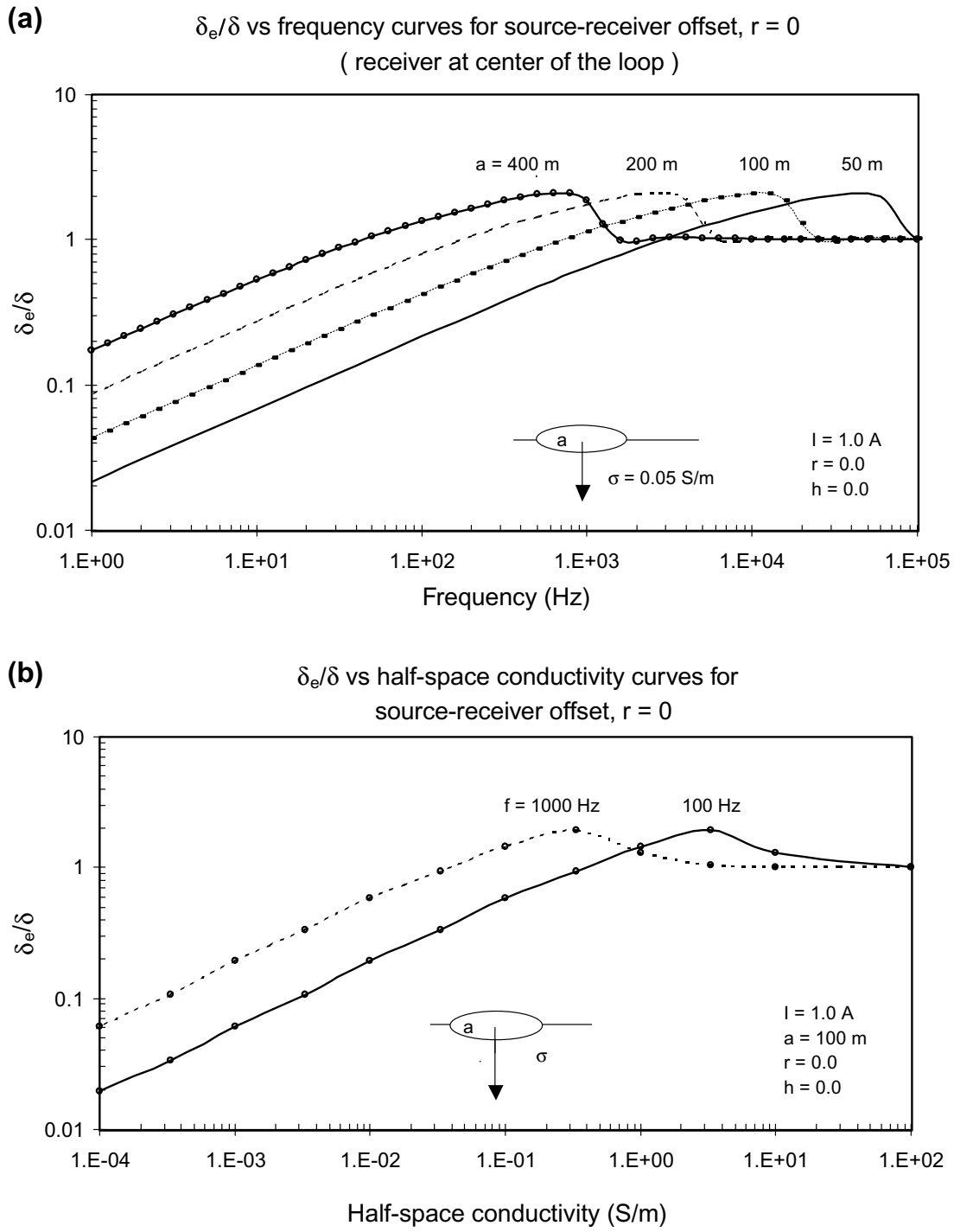


Fig. 4. Plot of normalized effective skin depth due to large circular loop source for source-receiver offset, $r = 0$ (i.e. receiver at center of the loop), and model parameters as shown in the figure, (a) $\delta_e/\delta$ versus frequency curves for varying loop sizes, and (b) $\delta_e/\delta$ versus half-space conductivity curves for frequencies 100 Hz and 1000 Hz.

sion, $\delta_e$ increases in general, because of increase in source moment. Further, with increase in loop dimension, the maximum peak shifts towards lower frequency region. The maximum value of $\delta_e/\delta$ attained for any frequency or loop size is higher for the source-receiver offset, $r = 2a$ as compared to that for $r = 0$. Moreover, from Fig. 5(b) it is observed that with increase in frequency, $\delta_e/\delta$ versus half-space conductivity curve shifts towards the lower conductivity region.

Figure 6 shows variation of $\delta_e$ with source-receiver offset for a horizontal electric dipole (length $ds = 1.0$ m and $I = 1.0$ A) for some selected frequencies and model parameters as shown in the figure. The plane wave skin depth $\delta$ is also shown for each frequency curve. From the figure, it is observed that $\delta_e$ curves show similar characteristic variation for all frequencies, and are also similar in shape to corresponding curves for the vertical magnetic dipole source as given in Reid and Macnae (1999). For small offsets, close to the dipole, $\delta_e$ is only a fraction of $\delta$. At these offsets, geometrical effects of the source dominate over the natural attenuation effect, and this portion of the curve exhibits variations

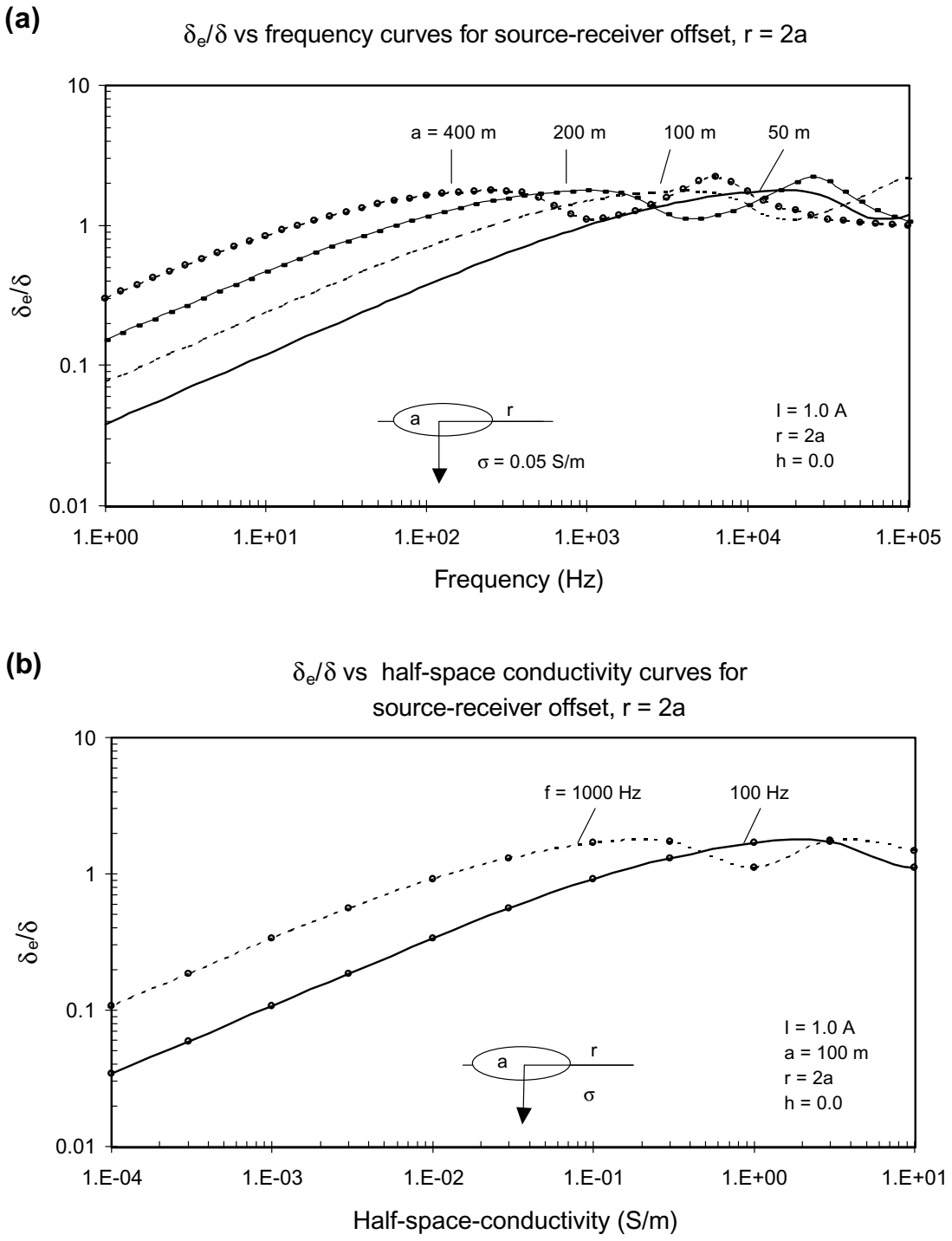


Fig. 5. Variation of normalized effective skin depth due to large circular loop source for source-receiver offset, $r = 2a$ and model parameters as shown in the figure, (a) $\delta_e/\delta$ versus frequency curves for different loop sizes, and (b) $\delta_e/\delta$ versus half-space conductivity curves for the frequencies 100 Hz and 1000 Hz.

characteristic to the source. Further, with increase in source-receiver offset, $\delta_e$ increases to its maximum value more than twice the plane wave skin depth $\delta$. Thereafter, it decreases and finally converges to $\delta$ for large offset values.

Figure 7(a) shows $\delta_e/\delta$ versus source-receiver offset curves for a horizontal electric dipole for varying half-space conductivity and survey parameters as shown in the figure, whereas Fig. 7(b) presents corresponding $\delta_e/\delta$ versus half-space conductivity curves for source-receiver offsets 300 m and 600 m for different survey and model parameters as shown in the figure. From Fig. 7(a), it is observed that with decrease in half space conductivity, there is an increase in source-receiver offset range in which $\delta_e$ exceeds the corresponding $\delta$. From Fig. 7(b), it is obvious that both the curves are similar to each other and are also similar to the corresponding curves for large loop sources (as in Fig. 4(b)). For small conductivity of the half space, $\delta_e$ is simply a fraction of $\delta$. With increase in conductivity $\delta_e$ increases and reaches to its maximum, and finally it converges to $\delta$ for high conductivity values. The effect of source-receiver offset is well

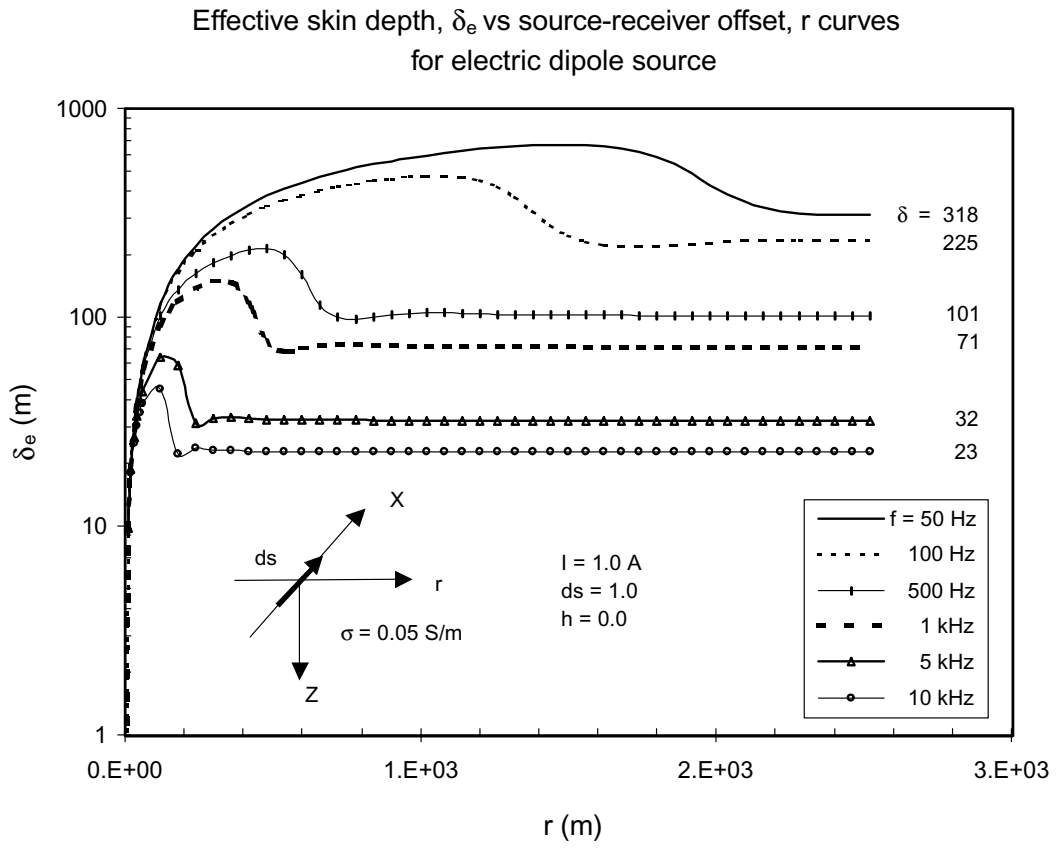


Fig. 6. Variation of effective skin depth, $\delta_e$ with source-receiver offset, $r$, for horizontal electric dipole (length $ds = 1.0$ m and $I = 1.0$ A) for selected frequencies and model parameters as shown in the figure.

noticed and with increase in source-receiver offset the curves shift towards lower conductivity region.

### 3.2 Discussion on effect of geometry and nature of source on $\delta_e$

Our results reveal that for small offsets, with receiver positions in close proximity of the source, $\delta_e$ curves show different variation for different sources, whereas for receiver positions away from the source ($2\delta < r < 8\delta$), the curves show similar variation for all sources, similar to that of a dipole source. This is due to the reason that at large offsets, large loop source behaves like a dipole source. Further, for receiver positions far away from the source, $\delta_e$ curves depict variation similar to a plane wave source. Thus, the $\delta_e$ curves in near vicinity of the source exhibit characteristic variation specific to the local source and depict effects of geometry and nature of the source. This can be noticed in $\delta_e$ versus source-receiver offset curves for the large loop source (as in Fig. 2) and horizontal electric dipole source (as in Fig. 6). This portion of the curve presents characteristic of the source.

A comparison of our results for the circular loop source with that of Reid and Macnae (1999) for a square loop source can only be done for offsets outside the loop, as there is no corresponding result for an in-loop point in Reid and Macnae (1999). For moderate to large offsets with receiver positions outside the loop, both curves show similar behavior which is similar to those for a vertical magnetic dipole source, and for very large source receiver offsets, both curves converge to the plane wave skin depth curve. However, for large induction number, our results for $\delta_e$ due to circular loop source converges to the plane wave skin depth (up to 3 decimal digits), whereas corresponding Reid and Macnae (1999) result for the square loop source shows significantly large values of $\delta_e$ as compared to the plane wave skin depth, which they explained as artifact of the computing method.

## 4. Examples of Application

For illustrating the application of effective skin depth to survey design and data interpretation, we have considered some theoretical examples of survey design using the large circular loop and horizontal electric dipole sources with source-receiver arrangements as shown in Fig. 1. The objective of survey design is to decide the optimum survey parameters for detecting a conductive 1.0 S/m basement lying beneath the 50 m thick 0.05 S/m upper layer in the layered earth environment. For such source-receiver geometries (as shown in Fig. 1), the EM response of a 0.05 S/m half-space and 2-layer earth model comprising of 50 m thick 0.05 S/m upper layer overlying the conductive 1.0 S/m basement have been compared at different source-receiver offsets, namely at $r = 0$, $r = a/2$, and $r = 2a$, and loop dimensions for the horizontal circular loop source, and at different source-receiver offsets for the horizontal electric dipole source.

Figure 8(a) shows frequency sounding curves for the amplitude of $H_z$ field over the proposed half-space and 2-layer earth models due to a horizontal circular loop source for source-receiver offset, $r = 0$ (i.e. receiver at center of the loop) and source loop radius $a = 50$ m, 100 m and 200 m. From Fig. 8(a), it is observed that for smaller loop size,

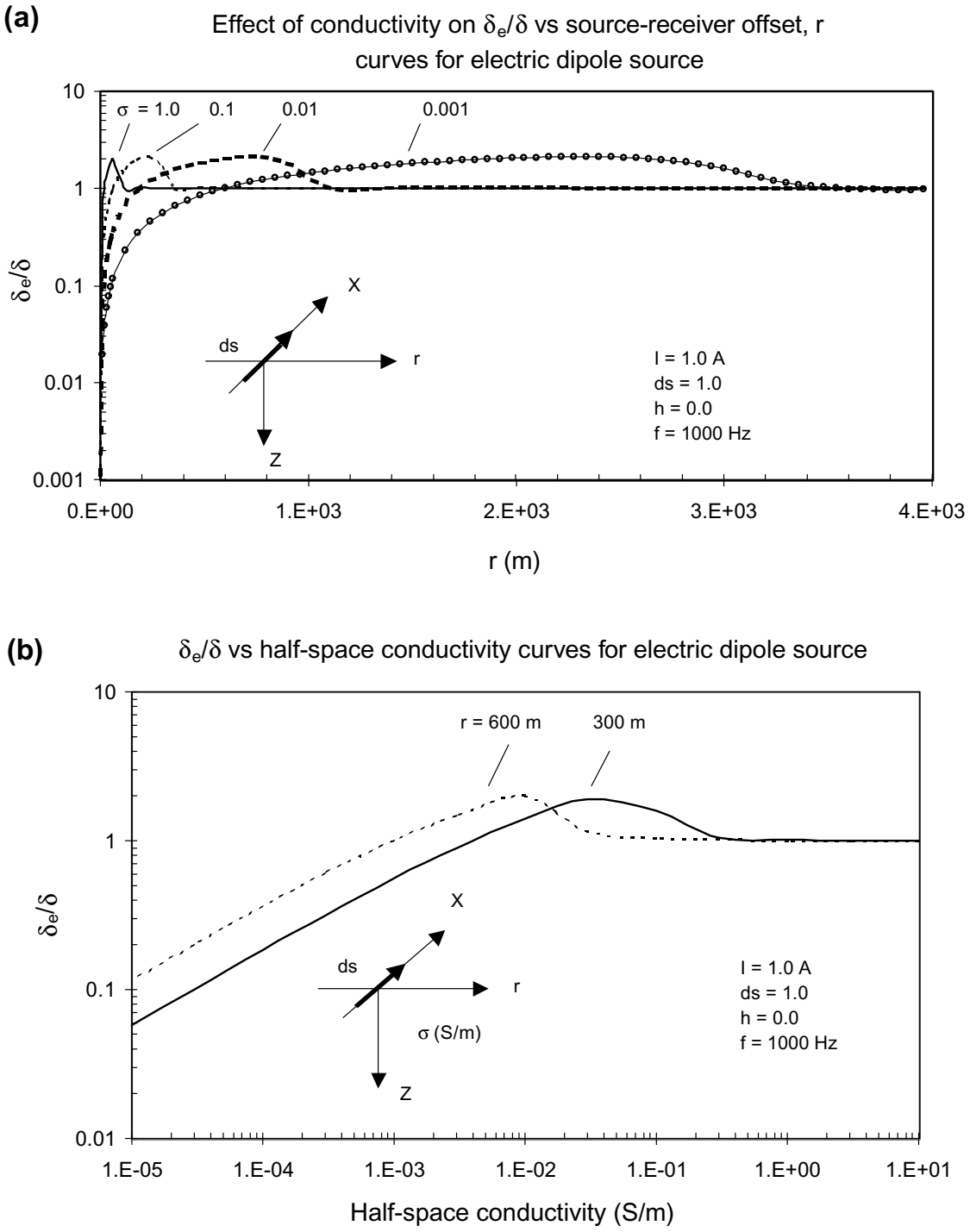


Fig. 7. Plot of normalized effective skin depth due to horizontal electric dipole (length $ds = 1.0$ m and $I = 1.0$ A) for model parameters as shown in the figure, (a) $\delta_e/\delta$ versus source-receiver offset curves for different conductivity values, and (b) $\delta_e/\delta$ versus half-space conductivity curves for source-receiver offset 300 m and 600 m.

$a = 50$ m, both the half-space and two layer curves are coincident at all frequencies, whereas for the loop size 100 m, there is clear difference (about 1% of the amplitude) between the half space and two layer response in the frequency range 50 Hz–2 kHz, and for those of loop size 200 m, there is a marked difference (more than 1% of the amplitude) between the half-space and two layer response for all frequencies less than 10 kHz. This behavior occurs due to the fact that for smaller loop size, the $\delta_e$ based on electric or magnetic field is less than the thickness of the overburden layer for all frequencies, and thus produces the same response for both the half space and two layer models, whereas for large loop sizes, it exceeds the first layer thickness at least for the lower frequency range and takes into account the effect of conductive basement, thus reflecting a marked distinction between the half space and two layer response. These results suggest that it is unlikely that a central loop EM sounding with loop radius $a = 50$ m would be able to detect the presence of basement in proposed 2-layer model, whereas the EM sounding with loop radius 100 m and 200 m would be able to de-

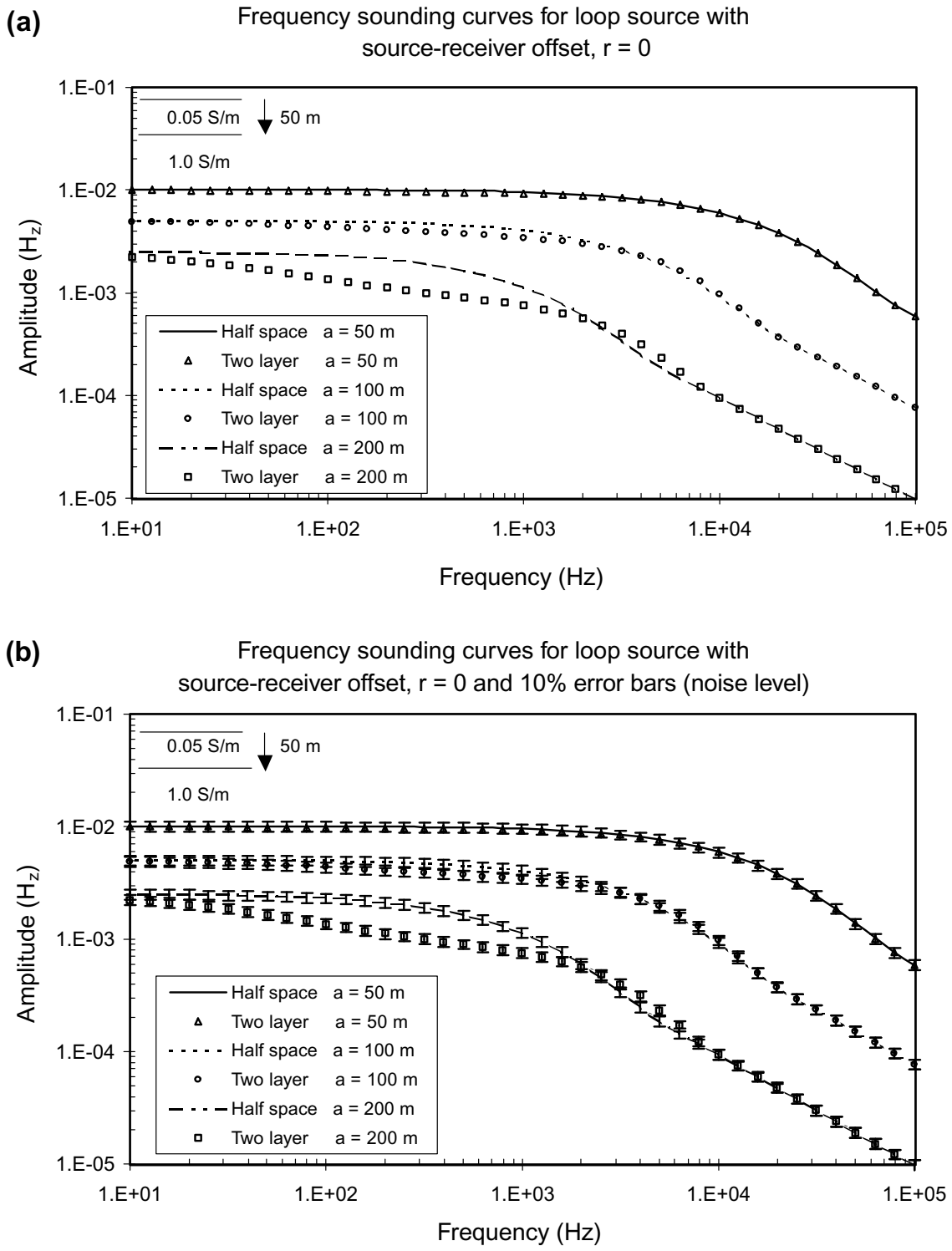


Fig. 8. Examples illustrating the relation of effective skin depth with observed EM response of a large circular loop source for source-receiver offset, $r = 0$. (a) Frequency sounding curves for amplitude of $H_z$ field over the half-space and 2-layer model under consideration (shown in figure) for the source loop radius $a = 50$ m, 100 m and 200 m, (b) Frequency sounding curves for amplitude of $H_z$ field over the half-space and 2-layer model (shown in figure) with 10% error bars for the source loop radius $a = 50$ m, 100 m and 200 m.

tect it at least in frequency range 50 Hz–2 kHz, and <10 kHz respectively. Interestingly, it is noticed that the frequency region in which the half space and 2-layer response curves differ significantly, nearly coincide with the frequency region in which $\delta_e$ exceed the plane wave skin depth, $\delta$. These results suggest that in order to detect a conductive basement using a central loop sounding, one can choose the optimum loop size in accordance with the source frequency and conductivity structure of the area.

Figure 8(b) presents the same sounding curves as shown in Fig. 8(a), with 10% error bars with objective of estimating the effect of noise level on interpretation and to get an idea about the real ability of this study for difficult field applications. From Fig. 8(b), it is observed that for smaller loop size,

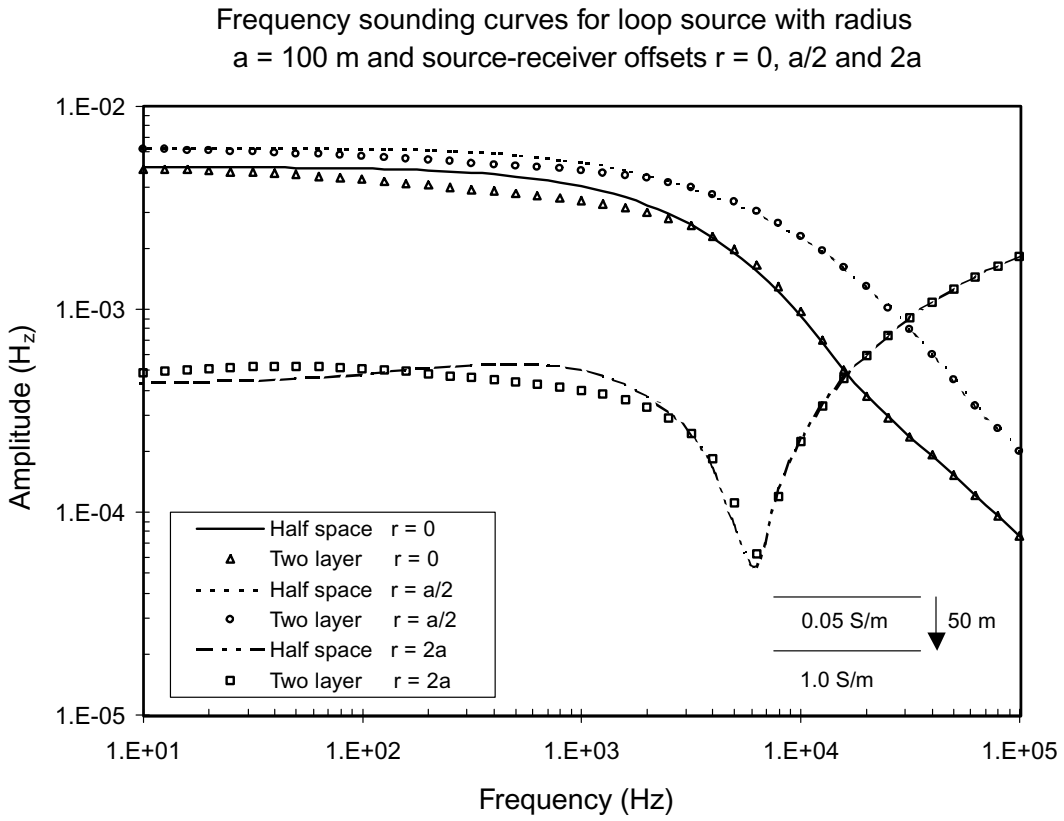


Fig. 9. Theoretical example illustrating the effects of effective skin depth on observed frequency sounding curves for amplitude of $H_z$ field, over the proposed half-space and 2-layer models due to large circular loop source at source-receiver offsets, $r = 0$, $a/2$ and $2a$, and its application to survey design and data interpretation.

$a = 50$ m, both the half space and 2-layer error bars are coincident for all frequencies, whereas for loop size 100 m, the two error bars, though not distinctly separated, are distinct in very small frequency range 300 Hz–800 Hz, and for the loop size 200 m, there is clear distinction between the half space and 2-layer error bars in the frequency range 30 Hz–1.5 kHz. These results depict that it is not possible to detect the conductive basement under consideration with 10% noise level using a loop of radius 50 m, whereas it might be possible to detect the basement using a loop of radius 100 m in a narrow frequency range 300 Hz–800 Hz, and a loop of radius 200 m in the wide frequency range 30 Hz–1.5 kHz. These results indicate that it is possible to get an estimation of loop radius and operating frequencies even with 10% noise level. A comparison of these results with those concluded from Fig. 8(a), depicts that noise level has significant effect on estimated survey parameters, and as a result the operating frequency range, in which conductive basement can be detected using the loop source of radius 100 m and 200 m, has been considerably reduced for the analysis presented with 10% noise level (error bars). In practice, if the noise level changes, then for deciding the optimum survey parameters, one should keep care of prevailing noise level arising from the instrument sensitivity and other noise factors.

Figure 9 shows frequency sounding curves for the amplitude of $H_z$ fields over the proposed half-space and 2-layer models due to a horizontal circular loop source of radius, $a = 100$ m and source-receiver offsets $r = 0$, $a/2$ and $2a$ respectively. From Fig. 9, it is observed that there is a marked difference between the half-space and two layer curves for all the three source-receiver offsets, which vindicates that the proposed basement in consideration can be easily detected using the horizontal circular loop source of radius 100 m at all the three source-receiver offsets under consideration. However, the frequency range for which half-space and two layer response show clear difference is broadest for the curves corresponding to $r = 2a$, followed by $r = 0$ and $r = a/2$. These results indicate that frequency range for which subsurface basement may be detected, is broadest for the source-receiver offset $r = 2a$ and narrowest for $r = a/2$. This is due to the reason that the $\delta_e$ due to a large loop source has maximum value for the offset, $r = 2a$ and minimum for $r = a/2$.

Figure 10 shows frequency sounding curve for the amplitude of $H_z$ field over the proposed half-space and 2-layer models for horizontal electric dipole source (length $ds = 1.0$ m and $I = 1.0$ A) for source-receiver offsets $r = 40$ m, 100 m and 200 m respectively. From figure, it is observed that for small offset 40 m, both half-space and 2-layer curves coincide with each other, whereas for large source-receiver offsets 100 m and 200 m, there is a marked difference (more than 1% of the amplitude) between the two curves. This is again due to the fact that for small offset, the effective skin depth is less than the thickness of the first layer and thereby produce the same response curves, whereas for large offsets it exceeds the first layer thickness and give rise to different response curves due to the effect of the conductive basement. These observations suggest that for detecting the basement

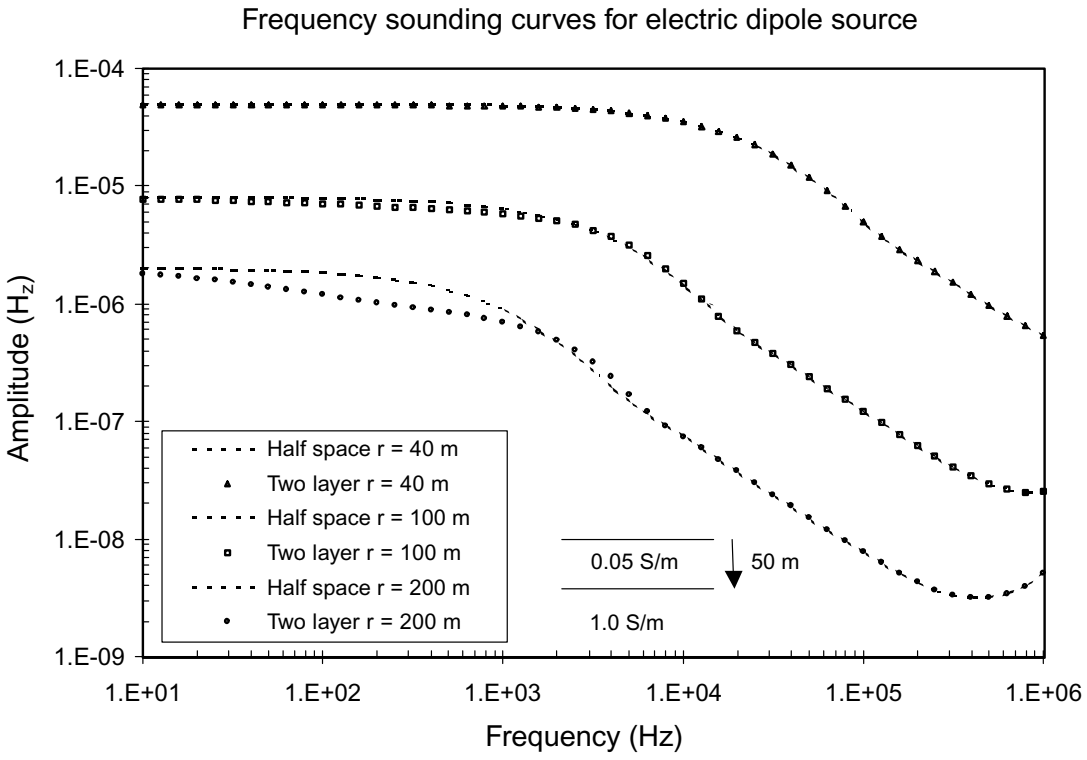


Fig. 10. Example demonstrating the effects of effective skin depth on observed frequency sounding curves for amplitude of $H_z$ field, over proposed half-space and 2-layer models due to a horizontal electric dipole source (length $ds = 1.0$ m and $I = 1.0$ A) for source-receiver offsets, $r = 40$ m, 100 m and 200 m, and its application to survey design and data interpretation.

using the horizontal electric dipole source, it is advisable to use the source-receiver offset 100 m or 200 m, instead of 40 m.

The overall analysis demonstrate that the information on $\delta_e$ can be used as an aid for selecting the optimum parameters in survey design, and setting the initial model parameters in inversion and data interpretation, in association with knowledge of geology and instrument sensitivity.

## 5. Conclusions

A detailed study of effective skin depth of EM fields due to large circular loop and horizontal electric dipole sources was performed to investigate the effects of survey and model parameters as well as for illustrating its application to survey design and data interpretation. The $\delta_e$ due to large circular loop or horizontal electric dipole source in a homogeneous half-space depends on source frequency, source moment and/or loop dimension, source-receiver offset and half-space conductivity. The variation of $\delta_e$ with source frequency exhibits similar trend as that of $\delta_e$ with half-space conductivity for both large loop and electric dipole sources. However, there is marked difference in $\delta_e$ values for the large loop and electric dipole sources in lower frequency or conductivity region. At low frequencies, $\delta_e$ is much lower than the plane wave skin depth, $\delta$. With increase in frequency, $\delta_e$ increases and exceeds the $\delta$, for medium to high frequencies, and finally it approaches to $\delta$ for very high frequencies. Similarly, at low conductivities, $\delta_e$ is only a fraction of $\delta$. With increase in conductivity, $\delta_e$ increases to its maximum, about $2\delta$, and finally it converges to $\delta$ for high conductivity values.

A comparative study of $\delta_e$ due to large circular loop and horizontal electric dipole sources reveals that in near vicinity of the source, the $\delta_e$ versus source-receiver offset curves depict variations characteristic to the local source, and exhibit different variation for different sources, whereas for receiver positions away from the source, $\delta_e$ versus source-receiver offset curves depict similar variation for all the sources. Finally, for receiver positions far away from the source, all curves depict variation similar to that of a plane wave skin depth curve. The effect of source on $\delta_e$ curves is manifested in close vicinity of source. For the large loop source, at the center of the loop, $\delta_e$ is normally less than the loop radius. Close to the loop circle, $\delta_e$ exhibits a sharp decrease in its value. Outside the loop, the $\delta_e$ increases and exceeds the plane wave skin depth, $\delta$ by factor of more than two at large offsets ($2\delta < r < 8\delta$) and, finally at very large offsets ($r > 10\delta$), it approaches to the plane wave skin depth, $\delta$. With increase in loop dimension, $\delta_e$ increases because the increase in source moment, whereas the maximum value of $\delta_e$ attained at moderate to large induction number decreases with increasing loop dimension. These results suggest that penetration of EM field depends on source moment, and thus a compact source of equal moment may penetrate to a depth greater than that due to the large loop source. The $\delta_e$ versus source-receiver offset curves for the electric dipole source depict their own characteristic variation. At small offsets, $\delta_e$ is simply a fraction of the $\delta$. With increase in offset $\delta_e$ increases and reaches to its maximum for moderate to large offset values, and finally it approaches to $\delta$ for large source-receiver offsets. With decrease in half-space conductivity, there is an increase in source-receiver offset range, in which $\delta_e$ exceeds the $\delta$. The results suggest that there is significant

effect of the nature and geometry of the local source on $\delta_e$ in near vicinity of the source.

From theoretical examples illustrating detectability of a conductive basement, it is evident that effective skin depth can be used successively for deciding the optimum survey parameters in real field problems. As the practical depth of investigation depends upon many factors including instrument sensitivity, noise level, signal strength and real field conductivity structure, so the $\delta_e$ must be used with care in association with other information about geology and instrument sensitivity. Thus, the information on effective skin depth can be used as an aid to survey design (for selecting survey parameters), and data inversion and interpretation (for setting initial model for inversion) in association with knowledge of local geology and instrument sensitivity.

**Acknowledgments.** The authors express their sincere thanks to reviewers Dr. Weerachai Siripunvaraporn and anonymous one, for their constructive and helpful comments, which greatly improved the original manuscript. One of the author (NPS) gratefully acknowledges the financial support provided by Japan Society for Promotion of Sciences (JSPS) for completion of this work in form of JSPS Post-doctoral fellowship for foreign researchers.

## References

Bostick, F. X., A simple almost exact method of MT analysis, Workshop on electrical methods in geothermal exploration, *U.S. Geol. Surv.*, contract no. 14080001-8-359, 1977.

Guptasarma, D. and B. Singh, New digital linear filters for Hankel $J_0$ and $J_1$ transforms, *Geophysical Prospecting,* **45**, 745–762, 1997.

Kaufman, A. A. and P. Hoekstra, *Electromagnetic Soundings,* 534 pp, Elsevier Science Publishing Co., Amsterdam, 2001.

Keller, G. V., Natural-field and controlled-source methods in electromagnetic exploration, *Geoexploration,* **9**, 99–147, 1971.

Parker, R. L., The existence of a region inaccessible to magnetotelluric sounding, *Geophys. J. Roy. Astr. Soc.*, **68**, 165–170, 1982.

Press, H. P., S. A. Teukolsky, W. T. Vetterling, and B. P. Flannery, *Numerical Recipes in Fortran (second edition),* 934 pp., Cambridge University Press, Cambridge, 1992.

Pridmore, D. F., Three dimensional modeling of electric and electromagnetic data using finite element method, Ph.D. thesis, Univ. of Utah, 1978.

Reid, J. E. and J. C. Macnae, Doubling the effective skin depth with a local source, *Geophysics,* **64**, 732–738, 1999.

Singh, N. P. and T. Mogi, EMLCLLER—A program for computing the EM response of a large loop source over a layered earth model, *Computer and Geosciences,* 2003 (in press).

Spies, B. R., Depth of investigation in electromagnetic sounding methods, *Geophysics,* **54**, 872–888, 1989.

Stratton, J. A., *Electromagnetic Theory,* McGraw-Hill Book Co., New York, 1941.

Wait, J. R., *Geo-electromagnetism,* Academic Press, New York, 1982.

Ward, S. H. and G. W. Hohmann, Electromagnetic theory for geophysical applications, in *Electromagnetic Methods in Applied Geophysics, Theory—Volume 1,* edited by M. N. Nabighian, pp. 131–308, SEG, Tulsa, Oklahoma, 1988.

N. P. Singh (e-mail: singhnpbhu@yahoo.co.in) and T. Mogi (e-mail: tmogi@eos.hokudai.ac.jp)